A Filippov Framework for a Conceptual Climate Model

Barry, A.M., McGehee, R. and Widiasih, E.

April 19, 2018

Abstract

In this article we develop a conceptual climate model based on Earth's energy balance that incorporates ice-albedo and greenhouse gas feedback effects. The resulting model is nonsmooth due to physical constraints on the ice line: it cannot extend beyond the pole or the equator. Because there is no general framework for this type of model, we extend the vector field to the nonphysical region so that we can use the machinery developed by Filippov [7]. Within this framework, we find that the physical region is forward invariant, and that sliding motion occurs on the physical boundary. In addition, we are able to prove that when greenhouse gas dynamics are sufficiently slow in comparison to the motion of the ice line the system exhibits a globally attracting periodic orbit which is reachable in finite time. This orbit can oscillate between wildly different scenarios including fully glaciated, partially glaciated, and ice-free states.

1 Introduction

There is significant evidence that large glaciation events took place during the Proterozoic era (2500-540 million years ago). In particular, this evidence points to the existence of glacial formations at low latitudes, see the review articles [10, 21] and the references therein. One theory on the exodus from such an extreme climate was put forward by Joseph Kirschvink [13], who advocated that there was accumulation of greenhouse gases in the atmosphere, eg. CO_2. His theory purports that during a large glaciation chemical weathering processes would be shut down, thus eliminating a CO_2 sink. Moreover, volcanoes would remain active during the glaciated state. The combination of these effects would lead to enough build-up of atmospheric carbon dioxide to warm the planet and start the melting of the glaciers, which would then melt rapidly due to ice-albedo feedback.

The mathematical models of so-called "snowball" events have been explored by many. In 1969, Mikhail Budyko and William Sellers independently proposed Energy Balance Models (EBMs) capturing the evolution of the temperature profile of an idealized Earth [2, 23]. Many others, for example [3, 1, 20], have followed in Budyko and Seller's footsteps and used similar conceptual models capable of exhibiting snowball events.

From the point of view of dynamical systems, many of these early works share a similar theme by focusing on a bifurcation analysis when the radiative forcing parameter, one that depends on changes in the atmospheric CO_2 and other greenhouse gases levels, is varied. The reader may find figures similar to those displayed in Figure 1 in earlier works [1, 10, 22]. These figures illustrate the state of Earth's glaciation in terms of atmospheric CO_2. In all of these figures, the effect of the radiative forcing due to CO_2 and other greenhouse gases is treated statically as a parameter in a simple bifurcation analysis.

Since glacial extent varies over time and dynamic processes such as chemical weathering affect the level of atmospheric CO_2, the bifurcation diagrams in Figure 1 could can be viewed as phase planes with dynamic variables consisting of the glacier extent (ice line) and radiative forcing due to greenhouse gases. In particular, if a global glaciation did occur, and Kirschvink's argument about the accumulation of atmospheric CO_2 held, then we should expect orbits of this dynamical system to traverse the extreme ice latitudes, ie. the equator (0^o) and the pole (90^o). We will see that the mathematical analysis of such a system requires sophistication beyond a bifurcation analysis.

The goal of this article is twofold: first, to extend existing energy balance models to include a dynamic greenhouse gas component, and second, to perform a rigorous analysis on the resulting nonsmooth model. The model extension is based on Kirschvink's idea that a chemical weathering shutdown would lead to accumulation of atmospheric greenhouse gases. We find that the physical restrictions on the ice line lead to a system which is piecewise Lipschitz continuous and can be analyzed using the perspective of Filippov.

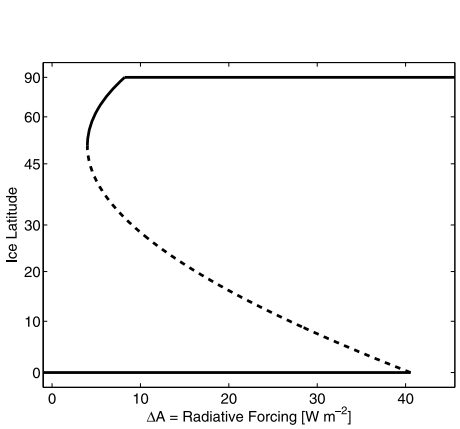

(a) A bifurcation diagram in Abbot, et al [1]

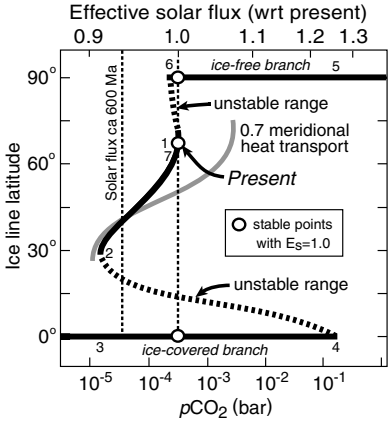

(b) A bifurcation diagram from Figure 6 in Schrag, et al [10]

Figure 1: Bifurcation diagrams found in previous models of snowball Earth.

We present the topics as follows. In the next section, we introduce some background motivating the model of interest. In Section 3, we discuss the Filippov framework for solutions to differential equations with discontinuous right hand sides. We show that an ice line model based on the Budyko EBM coupled with a simple equation for greenhouse gas evolution can be embedded in the plane to form a slow-fast system that has unique forward-time Filippov solutions. We then state and prove our main results about this system. In Section 4 we apply the result to a variant of our model and suggest a proof of concept for special rock formations called *banded iron*. We close the article with a discussion and ideas for future work.

2 The Equations of Motion

2.1 The Budyko Energy Balance Model and the Ice Line Equation

The Budyko Energy Balance Model (EBM) describes the evolution of the annual temperature profile $T = T(y, t)$, where t denotes time and y denotes the sine of the latitude. The governing

equation may be written:

$$R\frac{\partial}{\partial t}T(y,t) = Qs(y)(1-\alpha(\eta,y)) - (A+BT(y,t)) + C\left(\int_0^1 T(y,t)dy - T(y,t)\right). \quad (1)$$

The main idea is that the change in temperature is proportional to the imbalance in the energy received by the planet. The amount of short wave radiation entering the atmosphere is given by $Qs(y)(1-\alpha(\eta,y))$, where Q is the total solar radiation (treated as constant), $s(y)$ is the distribution of the solar radiation and $\alpha(\eta,y)$ is the albedo at latitude y given that the ice line is at latitude η. The outgoing longwave radiation is the term $A+BT(y,t)$; it turns out that the highly complex nature of greenhouse gas effects on the Earth's atmosphere can be better approximated by a linear function of temperature than by the Stephan-Boltzmann law for blackbody radiation (σT^4), see the discussion in [9]. The parameter A is particularly interesting here, because it is related to greenhouse gas effects on the climate system, which we will describe further in Section 2.2. The transport term $C(\int_0^1 T(y,t)dy - T)$ redistributes heat by a relaxation process to the global average temperature. Assuming symmetry of the hemispheres, one may take $y \in [0,1]$ and $T(y,t)$ as a symmetric temperature profile over the interval $[-1,1]$, hence, an even function of y. A more detailed discussion of this model can be found in [26].

The evolution of the ice-water boundary, or what is often called the ice line, η, affects the albedo function $\alpha(\eta,y)$. One way to model this effect is to add an equation describing the evolution of η as done in [28]. In this work, the ice line evolution was viewed as slow relative to the atmospheric processes governing the temperature profile $T(y,t)$. Many authors, eg. [26] and [20], specify a critical ice line annual average temperature, T_c, above which ice melts, causing the ice line to retreat toward the pole, and below which ice forms, allowing glaciers to advance toward the equator. Based on this, the augmented ice line equation governing η may be written as:

$$\frac{d\eta}{dt} = \varepsilon(T(\eta) - T_c) \quad (2)$$

The two equations (1) and (2) form a slow-fast system with an integro-differential equation, where the phase space must contain the function space of the temperature profile. Therefore, the dynamics of this coupled system take place in some infinite dimensional space. The work by Widiasih in [28] treated the model in a discrete time framework and also showed the existence of a one-dimensional attracting manifold.

With the ansatz that $T(\cdot,y)$ is piecewise quadratic with discontinuity at the ice line, ie. $y=\eta$, McGehee and Widiasih in [18] showed the existence of a one-dimensional attracting invariant manifold, similar to that shown in [28]. The invariant manifold is parametrized by the ice line, thereby reducing the dynamics into a single equation as in (3).

$$\dot{\eta} = h(\eta) \quad (3)$$

with

$$h(\eta) := \varepsilon\frac{Q}{B+C}\left(s(\eta)(1-\alpha(\eta,\eta)) + \frac{C}{B}(1-\overline{\alpha}(\eta))\right) - \frac{A}{B} - T_c \quad (4)$$

where $\overline{\alpha}(\eta) = \int_0^1 s(y)\alpha(\eta,y)dy$.

In what follows, we use the invariant manifold result by McGehee and Widiasih [18] and couple the above ice line equation to an equation for atmospheric greenhouse gas evolution.

2.2 Incorporating Greenhouse Gases

Here, we make an argument for a very simple form of an equation for greenhouse gas evolution. In the Budyko and Sellers models [2, 23], the parameter A plays the important role of reradiation constant. The Earth absorbs shortwave radiation from the sun, and some of this is reradiated in the form of longwave radiation. The current value of A is measured using satellite data to be approximately $202\ W/m^2$ [9, 26].

However, throughout the span of millions of years, A is not constant, as the amount of heat reradiated to space depends crucially on greenhouse gases, especially carbon dioxide. In fact, it was posited in [3] that A behaves like a function of the logarithm of atmospheric carbon dioxide, measured in parts per million. In this same article, the authors derive an expansion for $A = f(\log(pCO_2))$, and $f'(\log(pCO_2))$ is negative and constant to leading order. Thus we expect that A varies inversely with the logarithm of carbon dioxide. This agrees with the intuition that adding carbon into the atmosphere decreases its emissivity, allowing less energy to escape into space.

Kirschvink postulated that prior to the global glaciation period, the land masses were concentrated in the middle and low latitudes, setting the stage for a glaciated Earth. Then 'On a snowball Earth, volcanoes would continue to pump CO_2 into the atmosphere (and ocean), but the sinks for CO2 silicate weathering and photosynthesis would be largely eliminated '[10, 13]. In more recent work, Hogg [11] put forth an elementary model for the evolution of greenhouse gases consistent with Kirschvink's theory. In short, he argued that the main sources for atmospheric CO_2 were due to an averaged constant volcanism rate and ocean outgassing. The main carbon dioxide sink was said to be due to the weathering of silicate rocks. For our purposes, it will be enough to work with volcanism and weathering. Let V denote the rate of volcanism, W the rate of weathering and note that W should depend on the location of the ice line, η, or more specifically the amount of available land and rock to be weathered. Putting this together we obtain

$$\begin{aligned}\frac{dA}{dt} &= -\widetilde{\delta}(V - W\eta), \quad \widetilde{\delta} > 0 \\ &= \delta\left(\eta - \frac{V}{W}\right), \quad \delta > 0\end{aligned}$$

Setting the parameter $\eta_c = \frac{V}{W}$ we obtain the greenhouse gas equation

$$\frac{dA}{dt} = \delta\left(\eta - \eta_c\right). \tag{5}$$

with $\delta > 0$. From here on, we let

$$g(A, \eta) := \left(\eta - \eta_c\right). \tag{6}$$

Allowing A to vary, we rewrite the right hand side of the ice line equation (4) as $h(A, \eta)$. As a result, we have a system of equations for A and η:

$$\begin{cases} \dot{A} = \delta g(A, \eta) = \delta\left(\eta - \eta_c\right) \\ \dot{\eta} = h(A, \eta) = \left[\frac{Q}{B+C}\left(s(\eta)(1 - \alpha(\eta, \eta)) + \frac{C}{B}(1 - \overline{\alpha}(\eta)) - \frac{A}{B}\right) - T_c\right] \end{cases} \tag{7}$$

where in the above system we have rescaled time in order to absorb the parameter ε into δ. To understand the relative sizes of ε and δ, we refer to Hoffman and Schragg's elucidation of the Snowball scenario in which they argue that the weathering took place at a much slower rate than

the ice-albedo feedback (see Fig. 7 on page 137 [10]). With this in mind, we assume $\delta \ll \varepsilon$.

The idea of packaging the essence of the long term carbon cycle into one simple equation is not novel, though it is consistent with earlier findings [6, 11, 17]. The novelty comes from connecting such an equation to an energy balance model and analyzing the dynamics of the coupled system. Indeed, the parameter A_{ex} on page 644 [17] is the variable η in equation (7) and it represents the effective area of exposure of fresh minerals. The coupling of the ice line η and the greenhouse gas variable A follows naturally.

The system we examine is singularly perturbed, with critical manifold given by $h(A, \eta) = 0$ and the motion near this cubic manifold (away from the fold points) given roughly by $\dot{A} = g(A, \eta)$, see [12] for a more general treatment. However, the cubic manifold extends beyond the physical boundaries $\eta = 0, 1$ and so we must create reasonable assumptions for projection of this motion onto the physical boundaries. Furthermore, η should slide along these boundaries, as demonstrated by the bifurcation diagrams in Figure 1. This will be guaranteed by first carefully extending the vector field to the whole plane, and utilizing Filippov's theory for the resulting nonsmooth system.

3 A Filippov System for a Glaciated Planet

Before we dive into the analysis of the coupled (A, η) system, we shall first build an intuition for the type of system of our focus and prove a general result for such a system. We then apply this result to an extended version of (7) and show that the extended non-smooth system admits globally attracting periodic orbits.

Various frameworks for analyzing non-smooth systems have been developed, eg. by Caratheodory, Rosenthal, Viktorovskii, Utkin [7, 5]. Here, we choose to use the framework developed by A.F. Filippov [7]. The details of the proofs of existence and uniqueness of Filippov type of solutions may be found in the book [8] or in the article [7]. For convenience, we adopt the notations and statements of theorems used in [4].

3.1 Some Background on the Perspective of Filippov

Filippov's framework allows for solutions of differential equations with set-valued vector fields. In particular, if two vector fields disagree at some smooth discontinuity boundary, one considers convex combinations of the two vectors corresponding to the limits of the vector field as the boundary is approached from below and above. Any choice of vector within this set of combinations is allowable from the perspective of Filippov. To make this rigorous, we first define the set-valued map which corresponds to these convex combinations.

Definition 3.1. ***(Filippov Set Valued Map)*** *Suppose that f is measurable and locally essentially bounded, the Filippov set valued map of f, denoted by $K[f]$ is defined as:*

$$K[f](x) := \bigcap_{\delta>0} \bigcap_{\mu(N)=0} \overline{co}\left(f\left(B_\delta(x) \backslash N\right)\right)$$

where $\overline{co}$ denotes the closure of the convex hull.

A *Filippov solution* is based on extending a (possibly) discontinuous vector field to its convexification, i.e. the Filippov set valued map.

Definition 3.2. ***(Filippov Solution)*** *An absolutely continuous function $x : [0, \tau) \to \mathbb{R}^n$ is a Filippov solution to a differential equation $\dot{x} = f(x)$ if for almost all $t \in [0, \tau)$, it satisfies the differential inclusion*

$$\dot{x} \in K[f](x).$$

As expected, on the region where the vector field f is continuous, the Filippov set valued map satisfies $K[f](x) = f(x)$. Therefore, on such a region the Filippov solution is the classical solution. This consistency result is due to the following theorem.

Theorem 3.3. ***(Consistency), page 25 [5]***
If $f(x) : \mathbb{R}^n \to \mathbb{R}^n$ is continuous, then the Filippov set-valued map of f is itself, ie.

$$K[f](x) = f(x)$$

.

Existence and uniqueness of a Filippov solution can be achieved through the notion of solutions to the differential inclusion of this Filippov set-valued map.

Theorem 3.4. ***(Existence and uniqueness), p. 511-512 [4]*** *Let $f(x)$ be measurable and locally essentially bounded. Assume that $x \in \mathbb{R}^n$, and that there exists γ_x and $\epsilon > 0$ such that for almost every $x_1, x_2 \in B_\epsilon(x)$,*

$$(\xi_1 - \xi_2)^T (x_1 - x_2) \leq \gamma_x \|x_2 - x_2\|_2^2 \tag{8}$$

holds for all $\xi_1 \in K[f](x_1)$ and $\xi_2 \in K[f](x_2)$. Then for any $x_0 \in \mathbb{R}^n$ the initial value problem $\dot{x} = f(x)$ with initial condition $x(0) = x_0$ has a unique Filippov solution for almost all $t \in [0, \tau)$.

Recall that in the classical theory of existence and uniqueness, a Lipschitz condition on the vector field is sufficient to guarantee uniqueness of a solution to an initial value problem. Equation (8) is called the essentially one sided Lipschitz condition and its role is similar to that of the classical sense, ie. to control the growth of the vector field, particularly at the point of discontinuity.

We now set the stage for the motion along the discontinuity boundary. Let Σ be the smooth boundary separating two regions S_+ and S_-. Suppose that the vector field f is measurable and bounded, and that its limiting vectors, denoted f^+ and f^-, respectively, exist when $x \in \Sigma$ is approached from S_+ and S_-. Let N be the normal direction to the surface Σ directed from S_- to S_+, while f_N^+ and f_N^- are the projections of f^+ and f^- onto N. Let $x(t)$ be a Filippov solution of the differential equation defined by f.

Theorem 3.5. ***(Sliding), page 512 [4]*** *Suppose that the vector function $x(t) \in \Sigma$ is absolutely continuous for $t \in [t_1, t_2]$. Suppose $f_N^- \geq 0$, $f_N^+ \leq 0$, $f_N^- - f_N^+ > 0$ for all $t \in [t_1, t_2]$. Then the solution x slides along Σ if and only if for almost all $t \in [t_1, t_2]$*

$$\dot{x} = f^0(x) \tag{9}$$

where

$$f^0(x) = \alpha f^+(x) + (1 - \alpha) f^-(x) \tag{10}$$

with

$$\alpha(x) = \frac{f_N^-(x)}{f_N^-(x) - f_N^+(x)}. \tag{11}$$

Theorem 3.5 is crucial for determining the right dynamics at the discontinuity boundary. For each x in the boundary, equation (10) picks the correct α, hence the correct linear combination that results in the correct time derivative to push the solution along the discontinuity boundary.

In the next two theorems, let $\Sigma_0 \subset \Sigma$ be an open neighborhood on the discontinuity boundary Σ with $x(t) \in \Sigma_0$ for all $t \in [t_1, t_2]$.

Theorem 3.6. ***(No Crossing), page 513 [4]*** *If $f_N^+ \leq 0$ at all points of Σ_0, then for $t_1 \leq t \leq t_2$ no solution can go out of Σ_0 into S_+. Similarly, if $f_N^- \geq 0$, then no solution can go out of Σ_0 into S_-.*

Theorem 3.7. ***(Crossing), page 513 [4]*** *If $f_N^+ > 0$ and $f_N^- > 0$ at all points in Σ_0, then any solution that touches Σ_0 does so at exactly one point. In particular, in this case it crosses from S_- to S_+. Similarly, crossing from S_+ to S_- happens when both projections onto the normal vector are strictly negative.*

3.2 Casting the Model in a Filippov framework

As mentioned previously, there is a physical constraint that the ice line η must lie between 0 and 1. However, the model as it stands does not take this into account. The natural choice is to assume that $\dot{\eta} = 0$ when η reaches one of these physical boundaries. More specifically, we should take

$$\dot{\eta} = \begin{cases} 0 & \{\eta = 0 \text{ and } h(A,\eta) < 0\} \text{ or } \{\eta = 1 \text{ and } h(A,\eta) > 0\} \\ h(A,\eta) & \text{otherwise} \end{cases}$$
$$\dot{A} = \delta(\eta - \eta_c)$$

The first equation forces η to stop at the physical boundary exactly when it is about to cross that boundary (i.e. when $\eta = 1$ and $h > 0$ or when $\eta = 0$ and $h < 0$). When this happens, η remains constant and A continues to evolve. As A evolves, so does the value of h and this results in the η equation "turning back on" as soon as h becomes negative on the upper boundary or positive on the lower boundary.

We expect the system to exhibit periodic orbits between ice-covered and ice-free states, but there is no general theory that can be readily applied to this type of model. Rather than proving from scratch in this nonstandard system the existence, uniqueness and Poincare-Bendixson theorems, we take the alternate approach of *extending* the vector field to the nonphysical region in such a way that we can immediately apply the machinery developed by Filippov. This extension has no physical basis; it is merely a mathematical tool that we use to obtain the expected physical results. The type of extension we will use is highlighted by the following theorem.

Theorem 3.8. *Let $G(x,y), H(x,y) : \mathbb{R}^2 \to \mathbb{R}$ be C^1 functions. Define the vector field on $\mathbb{R} \times \mathbb{R}$ as follows:*

$$(\dot{x}, \dot{y}) := \begin{cases} (G, -|H|) & \textit{when } y > 1 \\ \left(G, \frac{H-|H|}{2}\right) & \textit{when } y = 1 \\ (G, H) & \textit{when } 0 < y < 1 \\ \left(G, \frac{H+|H|}{2}\right) & \textit{when } y = 0 \\ (G, |H|) & \textit{when } y < 0. \end{cases} \tag{12}$$

Then, an initial value problem with time derivative (12) *has a unique forward-time Filippov solution. Furthermore, the strip $\mathbb{R} \times [0,1]$ is forward invariant.*

Proof. Since the system is piecewise Lipschitz continuous, hence measurable and essentially bounded, to show existence and uniqueness of Filippov solutions, we need only show that the one sided Lipschitz condition of Theorem 3.4 is satisfied by equation (12). Furthermore, since G and $|H|$ are Lipschitz continuous on the plane minus the discontinuity boundaries, we need only demonstrate the one sided Lipschitz condition at the discontinuity boundary.

There are two such discontinuity boundaries: $y = 0$ and $y = 1$. We consider a point z on the line $y = 1$. Let δ be small enough that $B_\delta(z)$ is a neighborhood containing only the set $\{(x, y) : y > 0\}$. Suppose that $z_2 = (x_2, y_2)$ is a point above the line $y = 1$ ie. with $y_2 > 1$ and $z_1 = (x_1, y_1)$ is a point below the line $y = 1$ ie. with $0 < y_2 < 1$. We consider $(F(z_2) - F(z_1))^T (z_2 - z_1)$ for the following two cases:

1. $H(z_1) \geq 0$, then $(F(z_2) - F(z_1))^T (z_2 - z_1) = (0, -|H(z_2)| - H(z_1))^T (x_2 - x_1, y_2 - y_1) < 0$, since $-|H(z_2)| - H(z_1) < 0$ and $y_2 - y_1 > 0$. Then inequality (8) is satisfied with $\gamma_x = 1$.

2. $H(z_1) < 0$, then $F(z_2) - F(z_1) = (0, -|H(z_2)| + |H(z_1)|)$. The second entry may be estimated further: $-|H(z_2)| + |H(z_1)| \leq |H(z_1) - H(z_2)| \leq k_H \|z_1 - z_2\|$ where k_H is the Lipschitz constant of the function H Then the inequality (8) is satisfied with $\gamma_x = k_H$.

A similar argument holds for the other discontinuity boundary, and therefore, system (12) satisfies the one-sided Lipschitz condition, guaranteeing existence and uniqueness of Filippov solutions. Finally, applications of Theorems 3.6 and 3.7 to both discontinuity boundaries show that the strip $\mathbb{R} \times [0, 1]$ is forward invariant. The forward invariance of the strip is, of course, thanks to the construction of the vector field in the vertical direction $-|H|$ above $y = 1$ and and $|H|$ below $y = 0$.

□

Armed with this result, we return to system (7). Recall that g and h are both C^1 functions over the plane. Henceforth, we consider the initial value problem in the state space $(A, \eta) \in \mathbb{R} \times \mathbb{R}$ endowed with the following piecewise Lipschitz vector field:

$$(\dot{A}, \dot{\eta}) := \begin{cases} (\delta g(A, \eta), -|h(A, \eta)|) & \text{when } \eta > 1 \\ (\delta g(A, \eta), \frac{h(A,1) - |h(A,1)|}{2}) & \text{when } \eta = 1 \\ (\delta g(A, \eta), h(A, \eta)) & \text{when } 0 < \eta < 1 \\ (\delta g(A, \eta), \frac{h(A,0) + |h(A,0)|}{2}) & \text{when } \eta = 0 \\ (\delta g(A, \eta), |h(A, \eta)|) & \text{when } \eta < 0 \end{cases} \tag{13}$$

with initial value $(A(0), \eta(0)) \in \mathbb{R} \times \mathbb{R}$.

An application of Theorem 3.8 shows that a unique forward-time Filippov solution to the initial value problem (13) exists. Furthermore, the forward invariance of the strip $\mathbb{R} \times [0, 1]$ ensures the physically relevant aspect of the ice line η. We have arrived at the following conclusion:

Corollary 3.9. *There exists a unique Filippov solution to* (13)*. Furthermore, solutions starting inside the strip* $\mathbb{R} \times [0, 1]$ *stay in the strip in forward time.*

Remark 3.10. *There are many possible ways of extending system* (7) *beyond the strip* $\mathbb{R} \times [0, 1]$*. The choice of extension as done in system* (13) *assures the following points:*

1. *The attracting nature of the strip* $\mathbb{R} \times [0, 1]$*.*

2. *The switching from sliding to crossing is entirely determined by zeroes of $h(A, \eta)$. This point is especially important in the modeling of the physical system, since h signals the ice line's advance or retreat and h should be "off" at the extreme ice line location (pole or equator) and should "turn back on" when the system has reduced or increased enough greenhouse gases.*

3. *The time derivative of the sliding mode is entirely determined by the governing function of the greenhouse gas effect, $g(A, \eta)$. Again, this aspect is especially important in the modeling of the physical system, since at the extreme ice line location (pole or equator), the ice-albedo feedback shuts off and the greenhouse gas effect is the only driver of the system.*

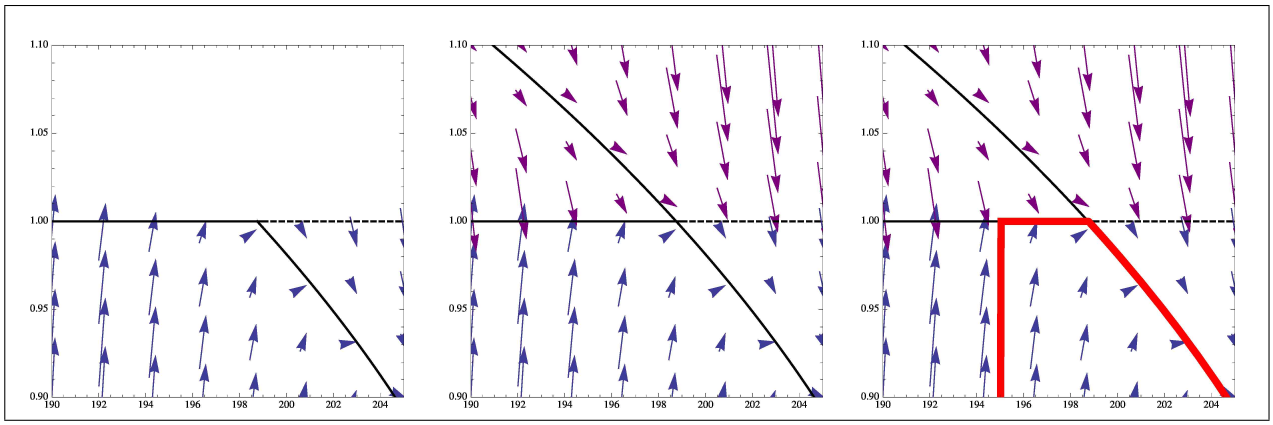

Figure 2: Close-up of (left) of the vector field near $\eta = 1$ in the physical region $\eta < 1$, the critical manifold (solid), and the physical boundary $\eta = 1$ which is solid or dashed based on its attractive or repelling nature. In the middle is our choice of extension beyond this boundary as well as the extension of the critical manifold to the nonphysical region $\eta > 1$. The image on the right includes a Filippov solution (red) exhibiting the induced sliding motion along the boundary as well as the crossing motion back into the physical region at the zero of h.

3.3 Main Result

As mentioned earlier, the system (13) is singularly perturbed with critical manifold defined by $h(\eta) = 0$. This is a cubic function of η with a single fold in $0 \leq \eta \leq 1$ at $\eta = \eta_p \approx 0.61$. Thus the system admits a single fixed point on this manifold for any choice of η_c. It is easy to check that the fixed point is stable when $\eta_c > \eta_p$ and unstable otherwise.

Denote the fold point by $\mathbf{p} = (\eta_p, A_p)$. We remark that $\mathbf{p}$ is a canard point in the sense of [16]. Therefore, for δ sufficiently small and η_c near, but below, the fold point the system undergoes a canard explosion. While mathematically interesting, planar canard orbits exist only for exponentially small parameter ranges which makes them unlikely observables. However, in higher-dimensional systems canards can be robust and more complex phenomena such as mixed-mode oscillations can occur. With this in mind, we remark that an interesting avenue for future research involves including an extra variable (w in [18]) and foregoing the invariant manifold reduction so that one can investigate the possible occurrence of canard-like behavior. For completeness we note that we expect that as η_c decreases through the Hopf bifurcation at η_p, the family of periodic orbits grows in amplitude, following the unstable branch of the slow manifold for longer and longer times, until it eventually collides with the boundary $\eta = 0$ in a sliding bifurcation. However, we do

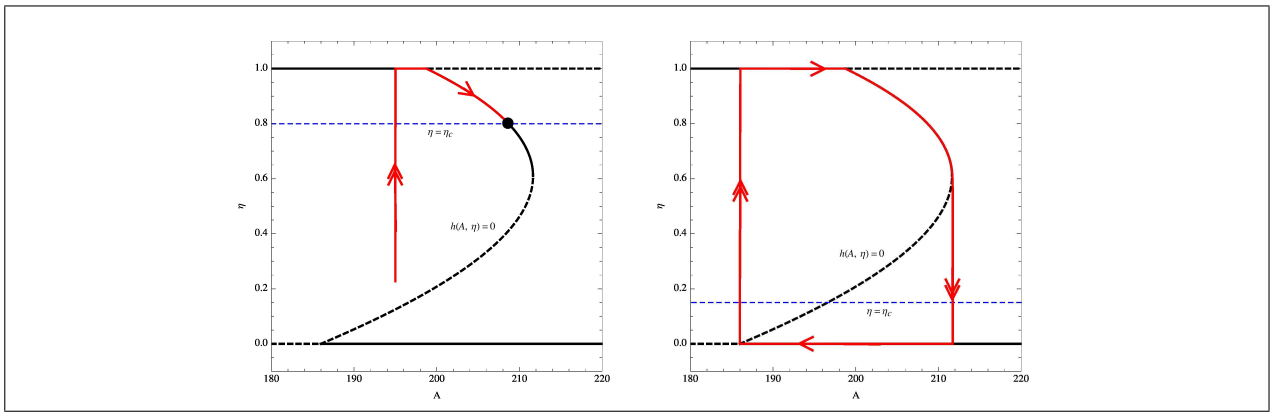

Figure 3: Phase space for the system (13). The image on the left shows a typical orbit of the system when $\eta_c = 0.8 > \eta_p$. On the right is a periodic orbit alternating between ice-free and ice-covered states when $\eta_c = 0.15$. The existence of such an orbit will be proven in Theorem (3.11)

not prove this here. Instead we are interested in periodic orbits that the system exhibits after the canard explosion. That is, when η_c is bounded away from, and below, η_p.

Theorem 3.11. *Choose $\eta_c < \eta_p$ outside the parameter range for which canard orbits occur. For $\delta > 0$ sufficiently small the initial value problem* (13) *has a unique, globally-attracting periodic orbit that is reachable in finite time and oscillates between $\eta = 0$ and $\eta = 1$, i.e. ice-covered and ice-free states.*

Proof. The proof relies on the construction of a trapping region, whose inner and outer boundaries can be seen in Figure (4). We begin by constructing the inner boundary, which is made up of the following 6 pieces:

(1) The segment of the critical manifold where $A_{q_1} < A < A_p$, which is made up of stable fixed points when $\delta = 0$. Here $\dot{\eta} = 0$ and $\dot{A} > 0$.

(2) The vertical line segment connecting the fold point $\mathbf{q}_p$ to the point (A_p, η_c). Here $\dot{\eta} \leq 0$ and $\dot{A} \geq 0$.

(3) The line segment connecting (A_p, η_c) to $(A_p - \sigma_1, 0)$, with σ_1 chosen so that the line segment does not intersect the critical manifold $h(\eta) = 0$. Here $\dot{\eta} < 0$ and $\dot{A} \leq 0$. We see that the vector field points "into" the trapping region (and out from the inner boundary) if $\left|\frac{d\eta}{dA}\right| = \left|\frac{\varepsilon h(\eta)}{\delta(\eta - \eta_c)}\right| > \frac{\eta_c}{\sigma_1}$. This can be achieved by choosing δ small enough.

(4) The horizontal line segment connecting $(A_p - \sigma_1, 0)$ to $\mathbf{q}_2$. On this region of the physical boundary the vector field points to the left.

(5) The line segment connecting $\mathbf{q}_2$ to a point $(A_{q_1} - \sigma_2, 1)$ where $\sigma_2 > 0$ is chosen such that the segment has positive slope. Here both $\dot{A}$ and $\dot{\eta}$ are positive. However, we can once again choose δ smaller if necessary so that the vector field points "into" the trapping region.

(6) The portion of the physical boundary $\eta = 1$ where $A_{q_1} - \sigma_2 \leq A \leq A_{q_1}$. Here the vector field points to the right.

The outer boundary of the trapping region can be constructed in a similar way, as can be seen in Figure (4). The constants $\sigma_4 > \sigma_3 > 0$ are chosen so that the line segment (i) does not intersect the critical manifold. The remaining constants are chosen to satisfy $\sigma_6 > \sigma_5 > 0$. Once these constants are chosen, δ will be made smaller if necessary on regions (i) and (iii).

Any orbit with initial condition outside the outer boundary of the trapping region must eventually reach the physical boundary $\eta = 0, 1$. Once on this boundary it will slide into the trapping region.

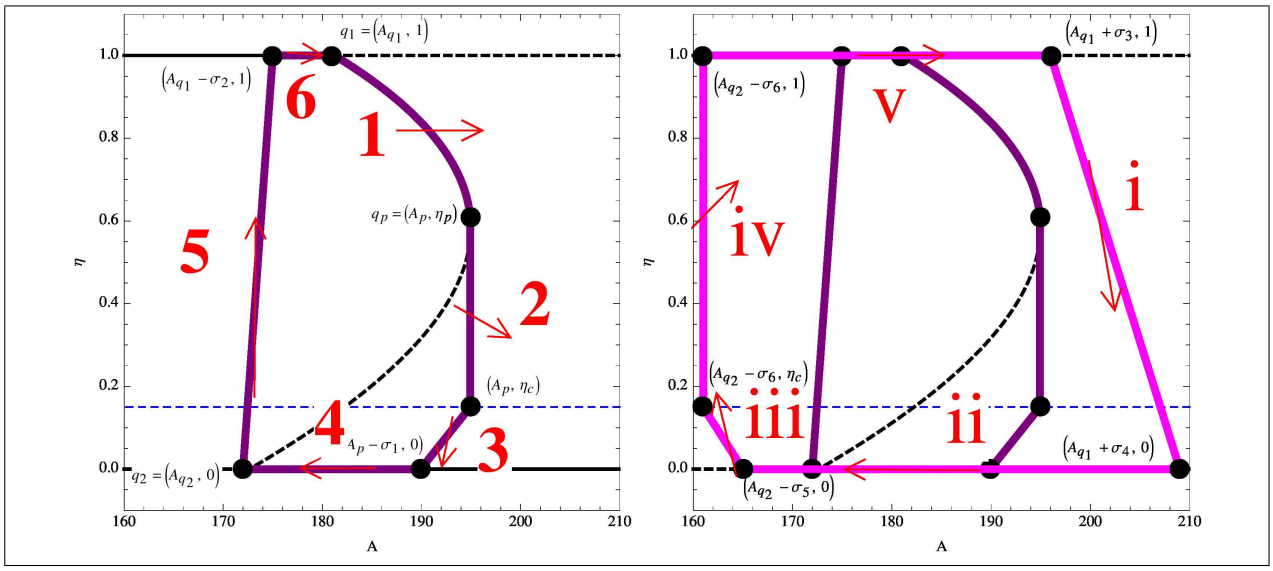

Figure 4: Inner (left) and outer (right) boundaries of the trapping region and the vector field on these boundaries (arrows).

Now consider an orbit with initial condition on the interior of the inner boundary of the trapping region. If this orbit reaches the physical boundary then it must enter the trapping region. Otherwise, it must stay on the interior of the physical region for all time in which case it must be bounded by a classical periodic orbit that is entirely contained within the strip, or more precisely within $\eta < \eta_p$, as there are no stable fixed points of the system. We compute the divergence of the vector field. Note that it is nonzero within the open region $\eta < \eta_p$:

$$\begin{aligned} \frac{\partial \dot{A}}{\partial A} + \frac{\partial \dot{\eta}}{\partial \eta} &= 0 + \frac{\partial \dot{\eta}}{\partial \eta} \\ &> 0, \quad 0 \leq \eta < \eta_p \\ &\leq 0, \quad \eta_p < \eta \leq 1. \end{aligned}$$

Thus any classical periodic orbit contained entirely in the region $\eta < \eta_p$ can be ruled out by Bendixson-Dulac's Criterion [25]. Moreover, any periodic orbit that contains points with $\eta > \eta_p$ must cross the critical manifold and enter the trapping region. Therefore we see that all orbits (except for the single fixed point) must enter the trapping region. Since any orbit that enters the trapping region must reach the physical boundary in finite time, it follows from forward-in-time uniqueness that it reaches a single periodic orbit in finite time. □

The previous occurrence of a complete snowball event is still a highly contested topic in geology. In the model (7), when $\eta_c > \eta_p$ the full system exhibits a small ice cap stable state. In the next section we present a variant of this system, as introduced by Abbot et al in [1]. By modifying the albedo function $\alpha(y, \eta)$ so that it differentiates between the albedo of bare ice and snow-covered ice, the new system has an additional stable state for an interval in η_c that corresponds to a large ice cap. In [1], this was called the *Jormungand* state because it consists of a snake-like band of open ocean at the equator.

4 The Jormungand state and banded iron formations

Rock formations called *banded iron* formed during the Neoproterozoic era. These consist mainly of thin (on the order of millimeters to centimeters in thickness) layers of chert and iron-oxide hematite [14]. There are multiple theories as to how these rocks came to be, see e.g. [15] [10]. One theory is related to the Snowball Earth Hypothesis: if Earth is ice-covered and the ocean largely anoxic then there will be an abundance of Fe ions with no oxygen to bond with. This could lead to accumulation of iron on the ocean sea floor or perhaps in coastal oases where bacteria may have survived during the snowball [21]. Due to a build-up of atmospheric carbon dioxide during the snowball, deglaciation could begin, allowing the iron-rich anoxic water to come into contact with oxygen. This would then result in layers of iron based on the amount of available oxygen, and hence banded iron. However, the periodic nature of the layers observed is largely unexplained. Could the variations be due to fluctuations of ice line at a time scale much shorter than the duration of the snowball Earth? Here we propose a "pulsating" Jormungand state - oscillations between Snowball and Jormungand states - as a mechanism for producing banded iron formations.

The new model is based on the assumption that the underlying albedo function distinguishes between ocean, bare ice, and snow-covered ice:

$$\alpha_J(y,\eta) = \begin{cases} \alpha_w, & y < \eta \\ \frac{1}{2}(\alpha_w + \alpha_2(\eta)), & y = \eta \\ \alpha_2(y), & y > \eta, \end{cases} \tag{14}$$

where $\alpha_2(y) = \frac{1}{2}(\alpha_s + \alpha_i) + \frac{1}{2}(\alpha_s - \alpha_i)\tanh M(y - 0.35)$ is as introduced in [1].

Here α_w is the albedo of open water, α_i is the albedo of bare sea ice, and α_s is the albedo of snow-covered ice. The model assumes sea ice aquires a snow cover only for latitudes above $y = 0.35$. We modify $h(A,\eta)$ by replacing α with α_J:

$$h_J(A,\eta) = \frac{Q}{B+C}\left(s(\eta)(1-\alpha_J(\eta,\eta)) + \frac{C}{B}(1-\overline{\alpha_J}(\eta))\right) - \frac{A}{B} - T_c \tag{14}$$

where we note that although α is only piecewise smooth, both $\alpha(\eta,\eta)$ and $\overline{\alpha_J}(\eta) = \int_0^1 \alpha(y,\eta)s(y)dy$ are smooth.

The critical manifold $\{h_J(A,\eta) = 0\}$ is plotted in Figure (5), along with an example of a "pulsating Jormungand" orbit. In fact, the existence of such an orbit can be proven using the same techniques as in Section 3 and so we close this section with a corollary to Theorem (3.11):

Corollary 4.1. *Consider the Filippov system* (13) *with Jormungand albedo, and choose η_c below the lower fold point and outside the parameter range for which canard orbits occur. The system has a unique, globally attracting periodic orbit that is reachable in finite time alternating between ice-covered and Jormungand states.*

Remark 4.2. *This modified system has other interesting orbits which we have not studied here because our main focus was on a proof of concept for banded iron formations. However, for the sake of completeness we point out that if the curve $\eta = \eta_c$ intersects the middle branch of unstable fixed points (again outside the regions for which canards can occur) then one can use the same techniques to prove the existence of a unique, globally attracting periodic orbit which alternates between Jormungand and ice-free states. An example of such an orbit can be seen below.*

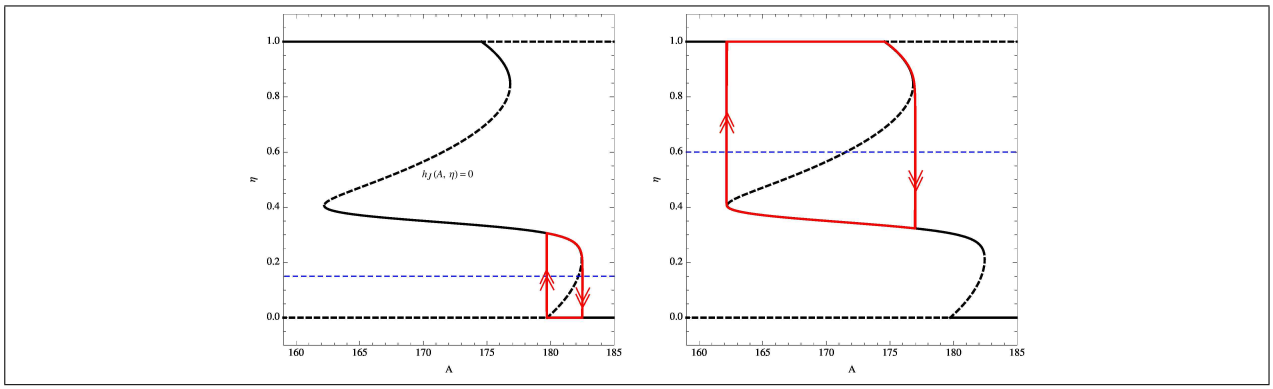

Figure 5: The critical manifold $\{h_J(A,\eta) = 0\}$ in black. Dashed lines correspond to unstable fixed points of the fast subsystem while solid lines represent stable fixed points. The nullcline $\eta = \eta_c(= 0.15)$ is in blue and the (left) pulsating Jormungand orbit is red. The system parameters for this simulation can be found in Appendix A. (Right) An example of an orbit oscillating between ice-free and Jormungand states.

5 Discussion and Future Directions

In this article we have extended a class of energy balance models to include a greenhouse gas component. The resulting system was nonsmooth due to physical constraints and did not immediately fit into any existing analytical framework. However, using an artificial tool (extending the vector field to the entire plane) we were able to fit the system into the Filippov framework and obtain exactly the expected motion. More specifically, we proved that the system exhibited periodic orbits between ice-free and snowball Earth states, thus verifying Kirschvink's hypothesis about carbon dioxide accumulation in a snowball scenario due to a shut down of chemical weathering processes [13]. We then applied our result to the case of Jormungand albedo and showed that it is possible to obtain oscillations between waterbelt and snowball states. In each case, we proved that the oscillations were both globally asymptotically stable and reachable in finite time. The latter was a consequence of the nonsmoothness of the model.

One general question brought about by this work has to do with building a general framework for such models so that we no longer need to appeal to artificial tools. A first step toward this framework might be a general theory for semiflows generated by smooth vector fields on manifolds with boundary.

It is also natural to ask how the shape of the critical manifold changes with parameters, e.g. could the lower fold in Figure (5) move to the left of the upper fold? We refer the reader to [27] for a number of examples. We leave for future study the periodic orbits the resulting system could produce.

Another interesting future direction is to study the explicit effect of the temperature (here we have considered it only through the equation for η based on the reduction by Mcgehee and Widiasih [18]) on the dynamics of the system. In a nonsmooth system, the addition of a stable dimension may destroy an existing stable periodic orbit [24]. Moreover, an additional dimension could result in more interesting glacial oscillations, such as mixed mode oscillations.

Acknowledgement: This research was supported in part by the Mathematics and Climate Research Network and NSF grants DMS-0940366, DMS-0940363. AB was also supported in part

by the Institute for Mathematics and its Applications with funds provided by the National Science Foundation. We thank the members of the MCRN Paleoclimate and Nonsmooth Systems seminar groups for many useful discussions, especially Mary Lou Zeeman and Emma Cutler. We also thank Andrew Roberts for his suggestions relating to the formulation of the problem.

A Parameters

The parameters used in simulations can be found in the tables below.

Parameter	Value	Unit	Source
Q	343	$Watts/m^2$	[26]
α_w	0.35	Dimensionless	[1]
α_i	0.45	Dimensionless	[1]
α_s	0.8	Dimensionless	[1]
B	1.9	$Watts/(m^2\ ^oC)$	[26]
C	3.04	$Watts/(m^2\ ^oC)$	[26]
T_c	-10	^oC	[26]
M	25	Dimensionless	[1]
$s(y)$	$s_0 + \frac{s_2}{2}(3y^2 - 1)$	Dimensionless	[19]
s_0	1	Dimensionless	[19]
s_2	-0.482	Dimensionless	[19]

Table 1: Parameters used to create the simulations in the figures

References

[1] D Abbot, A Voigt, and D Koll. The jormungand global climate state and implications for neoproterozoic glaciations. J. Geophys. Res., 116, 2011.

[2] MI Budyko. The effect of solar radiation variations on the climate of the earth. Tellus, 21(5):611–619, 2010.

[3] K Caldeira and JF Kasting. Susceptibility of the early earth to irreversible glaciation caused by carbon dioxide clouds. Nature, 359(6392):226–228, 1992.

[4] D Cheng, X Hu, and T Shen. Analysis of Nonlinear Control Systems, pages 509–532. Springer Berlin Heiderberg, 2011.

[5] J Cortes. Discontinuous dynamical systems. Control Systems, IEEE, 28(3):36–73, 2008.

[6] JM Edmond, MR Palmer, ET Brown, and Y Huh. Fluvial geochemistry of the eastern slope of the northeastern andes and its foredeep in the drainage of the orinoco in colombia and venezuela. Geochimica et cosmochimica acta, 60(16):2949–2974, 1996.

[7] AF Filippov. Differential equations with discontinuous righthand sides. American Mathematical Society Translations, 2:199–231, 1964.

[8] AF Filippov and FM Arscott. Differential Equations with Discontinuous Righthand Sides: Control Systems, volume 18. Springer, 1988.

[9] CE Graves, W-H Lee, and GR North. New parameterizations and sensitivities for simple climate models. J. Geophys. Res., 98(D3):5025–5036, 1993.

[10] P Hoffman and D Schrag. The snowball earth hypothesis: testing the limits of global change. Terra Nova, 14, page 129155, 2002.

[11] AM Hogg. Glacial cycles and carbon dioxide: A conceptual model. Geophys. Res. Lett., 35(1):L01701, 2008.

[12] CKRT Jones. Geometric singular perturbation theory. Dynamical systems, pages 44–118, 1995.

[13] J Kirschvink. Late proterozoic low-latitude global glaciation: the snowball earth. The Proterozoic Biosphere: A Multidisciplinary Study, pages 51–52, 1992.

[14] C Klein. Some precambrian banded iron-formations (bifs) from around the world: Their age, geologic setting, mineralogy, metamorphism, geochemistry, and origins. American Mineralogist, 90(10):1473–1499, 2005.

[15] KO Konhauser, T Hamade, R Raiswell, RC Morris, FG Ferris, G Southam, and DE Canfield. Could bacteria have formed the precambrian banded iron formations? Geology, 30(12):1079–1082, 2002.

[16] M Krupa and P Szmolyan. Extending geometric singular perturbation theory to nonhyperbolic points—fold and canard points in two dimensions. SIAM J. Math. Anal., 33(2):286–314, 2001.

[17] LR Kump, SL Brantley, and MA Arthur. Chemical weathering, atmospheric co2, and climate. Annual Review of Earth and Planetary Sciences, 28(1):611–667, 2000.

[18] R McGehee and E Widiasih. A quadratic approximation to budyko's ice albedo feedback model with ice line dynamics. SIAM J. Appl. Dyn. Sys., 13(1), 2014.

[19] GR North. Analytical solution to a simple climate model with diffusive heat transport. J. Atmos. Sci., 32(7):1301–1307, 1975.

[20] GR North. Theory of energy-balance climate models. J. Atmos. Sci, 32(11):2033–2043, 1975.

[21] RT Pierrehumbert, DS Abbot, A Voigt, and D Koll. Climate of the neoproterozoic. Annual Review of Earth and Planetary Sciences, 39:417–460, 2011.

[22] D Pollard and JF Kasting. Snowball earth: A thin-ice solution with flowing sea glaciers. J. Geophys. Res.: Oceans (1978–2012), 110(C7), 2005.

[23] WD Sellers. A global climatic model based on the energy balance of the earth-atmosphere system. J. Appl. Meteorol., 8(3):392–400, 1969.

[24] J Sieber and P Kowalczyk. Small-scale instabilities in dynamical systems with sliding. Phys. D, 239(1):44–57, 2010.

[25] SH Strogatz. Nonlinear dynamics and chaos (with applications to physics, biology, chemistry a. Perseus Publishing, 2006.

[26] KK Tung. Topics in mathematical modelling. Princeton University Press, 2007.

[27] J Walsh and E Widiasih. A dynamics approach to a low-order climate model. Discrete Cont. Dyn.-B, 19(1), 2014.

[28] ER Widiasih. Dynamics of the budyko energy balance model. SIAM J. Appl. Dyn. Sys., 12(4):2068–2092, 2013.